Supplementary information

Unravelling Chemical Heterogeneity and Dual Emission Pathways in Graphene Quantum Dots via Single-Particle Infrared Spectroscopy

Subhro Kundu,[a] Abu Bakar Siddique,[a] Irvin Fernando Guzmán González,[a] Kevin Armando Rodríguez Mireles,[a] Maritza Iveth Pérez Valverde,[a] Nicolás Antonio Ulloa Castillo,[a] Madhusoodanan Reghunathan,[c] Domingo Ixcoatl García Gutiérrez,[c,d] Eduardo Martínez Guerra,[b] and Mallar Ray [a]*

[a.] *School of Engineering and Sciences, Tecnológico de Monterrey, Monterrey, Nuevo León 64849, Mexico.*
[b.] *Centro de Investigaciones en Materiales Avanzados, CIMAV Unidad Monterrey, Alianza Norte 202, Apodaca, Nuevo León, C.P. 66628, Mexico.*
[c.] *Universidad Autónoma de Nuevo León, Centro de Innovación, Investigación y Desarrollo en Ingeniería y Tecnología, Apodaca, 66600, Nuevo León, México*
[d.] *Universidad Autónoma de Nuevo León, Facultad de Ingeniería Mecánica y Eléctrica, San Nicolás de los Garza, 66455, Nuevo León, México*

Section 1. AFM analysis

Sample Preparation

A colloidal dispersion of the sample in DI water was first prepared at a concentration of 1.1 mg/mL. This solution was then ultrasonicated for 30 minutes. Meanwhile, the top layer of the mica substrate was cleaved using adhesive tape. Subsequently, the solution was drop-cast onto the freshly cleaved mica. Finally, the substrate with the deposited sample was ultrasonicated for an additional 10 minutes to ensure well-distributed particles on the substrate.

Spatial Resolution of the PiFM

The Vista One PiFM equipment from Molecular Vista has a spatial resolution (topography) limited by the tip radius of curvature and the AFM scanner precision. As mentioned in the main document, the tip radius of curvature is 67 nm and, the scanner precision of the x, y and z axes is 100 pm RMS. Lateral resolution (xy) is limited by the tip shape and the features of the sample, the GQDs and NGQDs were placed on a flat surface, which helps with the lateral measurements; once the tip convolution is considered, an approximation of the true size can be resolved. Height resolution is only limited by the AFM scanner precision. In our samples, ~100 pm RMS is precise enough to measure sub-10 nm heights.

Small GQDs

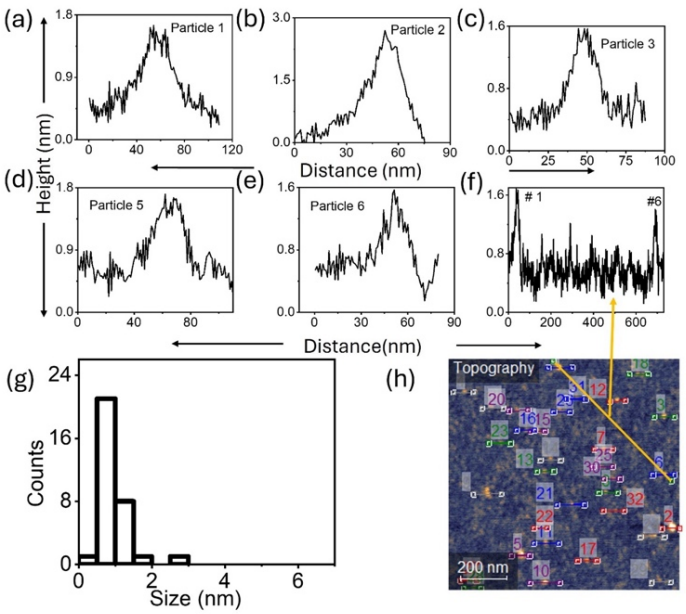

Figure S1: Particle height analyses of small GQDs. (a-e) Height profile of selected particles; (f) line profile over the chrome line indicated in (h) containing particle #1 and particle # 6 as marked in the AFM micrograph; (g) histogram showing the height distribution of the particles analysed; (h) AFM image with particle numbers and lines of small GQD.

Medium GQDs

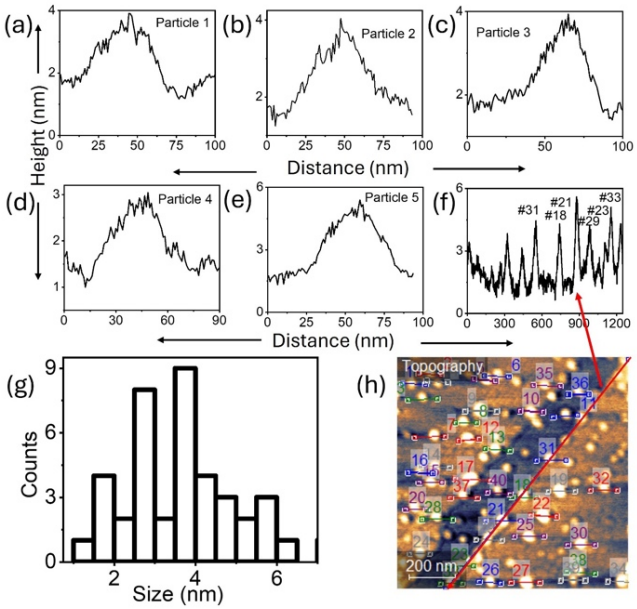

Figure S2: Particle height analyses of medium GQDs. (a-e) Height profile of selected particles; (f) line profile over the red line indicated in (h) containing several particles out of which particle #31, #18, #2, #29, #23 and #33 (as marked in the AFM micrograph) are indicated for easy reference; (g) Height distribution histogram of the particles; and (h) AFM image with particle numbers and lines.

Large GQDs

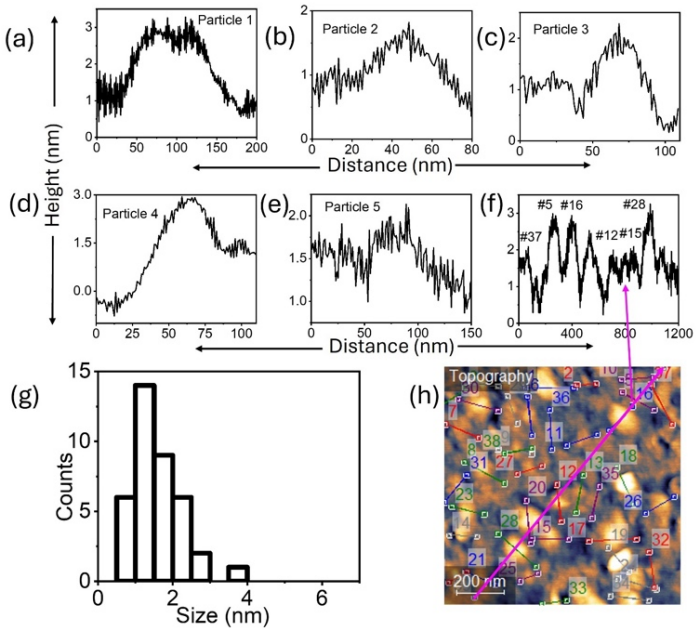

Figure S3: Particle height analyses of large GQDs. (a-e) Height profile of some selected particles, (f) line profile over the pink line indicated in (h) containing several particles out of which particle #28, #15, #12, #16, #5 and # 37 (as marked in the AFM micrograph) are indicated for easy reference, (g) histogram showing the height distribution of the particles; and (h) AFM image with particle numbers and lines of large GQD.

Small NGQDs

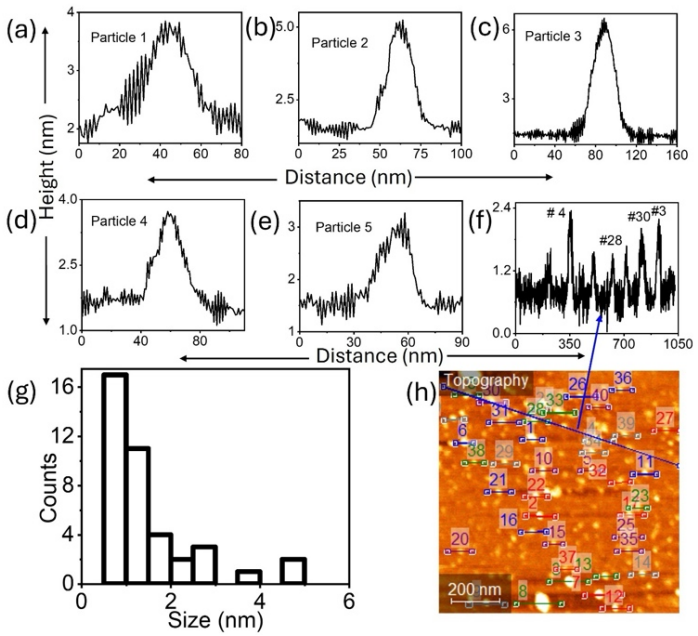

Figure S4: Particle height analyses of small NGQDs. (a-e) Height profile of selected particles, (f) line profile over the blue line indicated in (h) containing several particles out of which particle #3, #4, #28 and # 30 (as marked in the AFM micrograph) are indicated for easy reference, (g) histogram showing the height distributions of the particles; and (h) AFM image with particle numbers and line.

Medium NGQDs

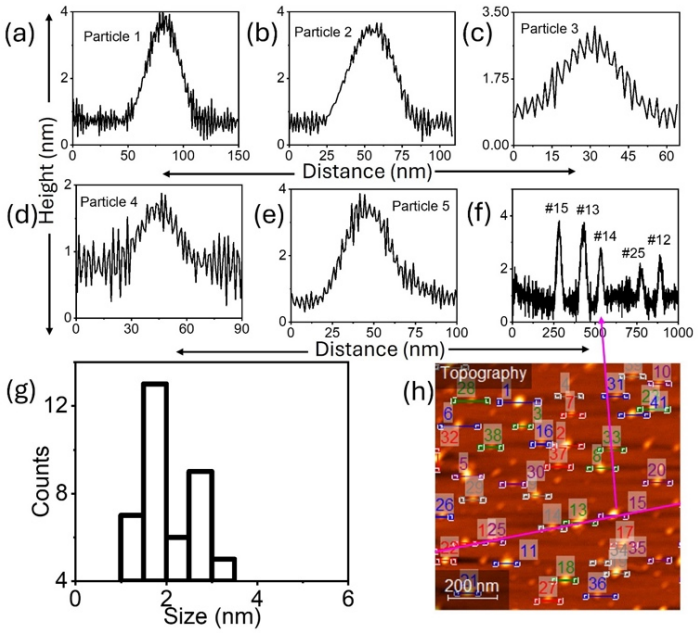

Figure S5: Particle height analyses of medium NGQDs. (a-e) Height profile of selected particles, (f) line profile over the pink line indicated in (h) containing several particles out of which particle #15, #13, #14, #25 and #12 (as marked in the AFM micrograph) are indicated for easy reference and (h) AFM image with particle numbers and lines.

Large NGQDs

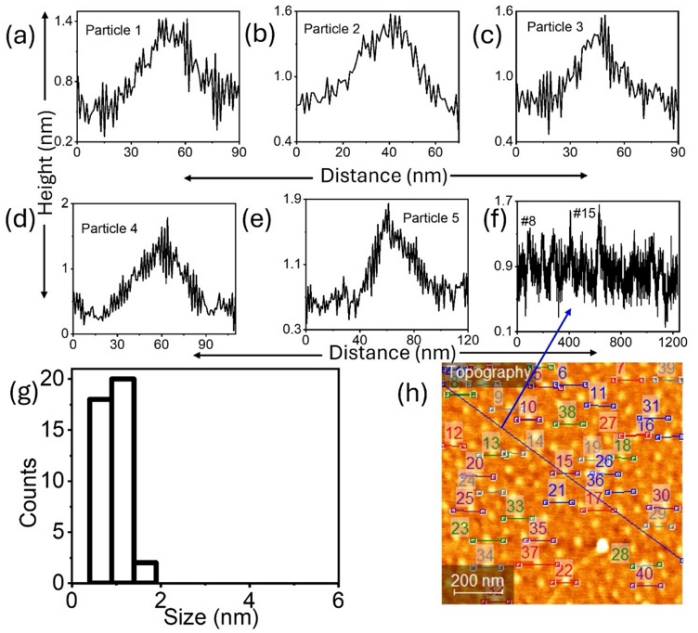

Figure S6: Particle height analyses of large NGQDs. (a-e) Height profile of selected particles, (f) line profile over the pink line indicated in (h) containing several particles out of which particle, #15 and #8 (as marked in the AFM micrograph) is indicated for easy reference, (g) histogram of height of the particles and (h) AFM image with particle numbers and lines of large NGQD.

Section 2. Tip deconvolution

The AFM tip used in this study had a radius of curvature of 67 nm. Since the average particle size measured were smaller than the tip radius, we used the following equation to correct for the tip convolution effect.[1]

$$S = 2 \times \left(R \times D + \frac{D^2}{4} \right)^{1/2}$$

Section 3: Chemical analysis

Spectral Resolution

The spectral resolution is 1 wavenumber, due to a high tuneable IR laser, specifically a QCL (Quantum Cascade Laser) from Block Engineering with a spectral range of 744-1884 cm^{-1}.

The Vista One PiFM is properly calibrated with well-known IR calibration samples such as polyethersulfone (PES), polymethyl methacrylate (PMMA), Nylon and AFM calibration samples made of silicon and silicon oxide.

Table S1: Correlation table for peaks, relative intensity, and position from PiF-IR spectra of the small GQD

Particle No. / Wavenumber	1	2	3	4	5	6	7	Group
1785	0	0	0	0.45	0	0	0.29	νC=O[2]
1779-1778	0.4	0	0	0	0	0	0	νC=O[3]
1775	0	0	0.47	0	0.12	0	0	νC=O[4]
1770	0	0	0	0	0	0	0.32	νC=O[4]
1765	0	0	0	0	0	0	0	νC=O[5]
1760	0	0	0	0	0	0	0	νC=O[6]
1755	0	0	0	0	0.13	0	0.31	C=O[7]
1749	0.57	0.39	0.39	0	0	0	0	νC=O[8]
1740	0	0	0	0	0	0	0	νC=O[9]
1734- 1732	0.85	0.56	0.55	0.51	0.16	0.45	0.44	νC=O[10]
1730	0	0	0	0	0	0	0	νC=O[11]
1720-1718	0.57	0.41	0.45	0.5	0	0.39	0.37	νC=O[12,13]
1700-1699	1	0.9	0.5	1	0.18	0.48	0.52	C=O[14]
1690	0	0	0	0.43	0	0	0	C=O[15]
1685-1680	0.77	0	0.4	0.48	0	0.35	0	νC=C[16]
1676-1675	0	0	0	0.44	0	0	0.3	$\nu_{as}HCO_3^-$ [17]
1669	0.4	0	0	0.54	0	0	0	νC=O[18]
1654	0.62	1	1	0.64	1	1	1	νC=C[6]
1640	0.64	0	0	0.47	0.13	0.29	0	νC=O[19]
1630	0	0.42	0	0.51	0.14	0.36	0.41	νC=C[20]
1629	0.69	0	0.52	0	0	0	0	νC=C[20]
1625-1623	0.65	0	0	0	0	0	0	δOH[21]
1620-1619	0.49	0	0.59	0	0	0	0	νC=C[22]
1600	0	0	0	0	0	0.31	0.29	C=O/C=C[23]
1590	0	0	0	0	0.11	0	0	νC=C[24]
1585	0.49	0.61	0	0.58	0	0	0	νC=C[25]
1570	0.56	0	0	0	0.14	0	0	νC=C[26]
1565	0	0.65	0	1.44	0	0	0.26	νC=C[27]
1560	0	0	0	0.58	0	0.34	0	νC-C[28]
1550	0	0.4	0	0.58	0	0	0.34	νC=C[29]
1545	0	0	0.37	0	0.14	0	0	νC=O[29]
1540	0	0	0	0	0	0.38	0	C=C[30]
1535	0	0	0	0	0	0	0.23	νC=C[31]
1529-1528	0	0	0	0.45	0	0	0	νC=C[32]
1510-1509	0	0.42	0	0.46	0	0	0.2	νCOO-[33]
1505-1504	0	0	0	0	0	0	0	νC=O[34]
1485	0	0.44	0	0.42	0	0	0	νC=C[35]
1474	0.45	0	0	0	0	0	0	ν/δCH[36]
1475-1472	0	0	0	0	0	0	0.27	ν_sC-O[37]
1470	0	0	0	0.45	0	0	0	ν_{sym}C-O[37]
1460-1459	0	0	0.43	0	0.14	0.33	0.4	νC=O[38]
1445	0.55	0	0	0	0.149	0	0	$\nu_{sym}HCO_3^-$ [17]
1440-1439	0.53	0	0	0	0.143	0	0	δCH_3[39]

1420-1419	0	0	0	0	0	0	0.28	COO^- [40]
1415-1414	0	0	0	0	0	0	0	νC-H[41]
1380-1379	0	0	0	0	0.149	0.34	0	CO_3^{2-} [18]
1374	0.53	0	0	0	0	0	0	δOH[42]
1369-1368	0.421	0	0	0	0	0	0.38	βOH[43]
1220	0.39	0.20	0.26	0.24	0.08	0.15	0.15	COC[44]

Table S2: Correlation table for peaks, relative intensity, and position from PiF-IR of the medium GQD.

Particle No. / Wavenumber	1	2	3	4	5	6	7	Group
1774	0	0	0	0	0.07	0	0.08	νC=O[45]
1742	0	0.07	0	0	0.06	0	0.07	νC=O[9]
1734- 1732	0	0	0	0	0	0.11	0	νC=O[10]
1695	0.56	0.22	0.29	0.55	0.22	0.68	0.38	νC=O[6]
1684-1680	1	1	1	1	1	1	1	νC=C[16]
1670-1669	0.09	0	0.08	0.08	0.07	0.1	0.07	C=O[46]
1643-1641	0	0	0	0	0	0.11	0	νCH=O[47]
1646-1645	0	0.06	0.08	0	0	0	0	HC=O[48]
1634	0	0.06	0	0.08	0	0	0	C=O-H[49]
1623-1622	0	0.07	0.07	0	0.07	0	0	δOH[50]
1594	0	0	0	0	0.06	0	0	C=C [51]
1564	0	0	0	0	0.06	0	0	νC=C [52]
1547	0	0	0	0	0.07	0	0	νC=C [53]
1509	0	0	0	0	0.05	0	0	νCOO^- [33]
1472	0	0.06	0	0.07	0.06	0.11	0	ν_sC-O[37]
1459	0	0	0	0	0	0.12	0	νC=C[54]
1456-1455	0	0	0.07	0.08	0.08	0	0.06	OH[55]
1441-1440	0	0	0	0	0	0	0.06	δCH[56]
1423	0	0	0	0	0	0	0.06	δOH[57]
1420	0	0	0	0.07	0.06	0.12	0	COO^- [40]
1398	0	0	0	0	0	0	0.06	νC=C[54]
1369-1368	0	0	0	0	0.06	0	0	βOH[43]
1375	0	0	0	0.06	0	0	0	OCHO[58]
1361	0	0	0	0	0	0	0.05	νC-O[59]
1338	0.06	0	0	0	0	0	0	δ/νOH[60]
1337-1336	0	0	0	0	0	0.06	0	CH_3CH_2O[61]
1284	0	0	0	0	0.04	0	0	νC-O Aromatic [62]
1262-1260	0	0	0.06	0.06	0	0.09	0.07	νC-O[63]
1258-1256	0.08	0.44	0	0	0	0	0	ν_{as}COC[64,65]
1254	0	0	0	0	0.05	0	0	νC-O[66]

Table S3: Correlation table for peaks, relative intensity, and position from PiF-IR of the large GQD.

Particle No. / Wavenumber	1	2	3	4	5	6	7	Group
1778	0.06	0	0	0	0	0	0	νC=O[3]
1760-1759	0.08	0	0	0	0	0	0	νC=O[6]
1742	0.09	0.1	0.09	0.13	0.09	0.11	0.11	νC=O[9]

1734	0	0.06	0.07	0.08	0	0	0	νC=O[10]
1710	0	0.06	0.07	0.1	0	0	0	COOH[67]
1695	0.23	0.22	0.27	0.35	0.25	0.28	0.23	νC=O[6]
1684-1680	1	1	1	1	1	1	1	νC=C[16,46]
1669	0.08	0.09	0.08	0.11	0.09	0.1	0.09	C=O[68]
1643	0	0.07	0	0	0	0	0	νCH=O[47]
1638	0.08	0	0	0	0	0	0	νC=C[49]
1634	0	0	0.08	0	0.08	0	0	C=O-H[49]
1585	0	0	0	0	0	0.07	0	νC=C[25]
1557	0	0	0	0	0.06	0	0	νCH[69]
1568	0.06	0	0	0	0	0	0	νCOOH[61]
1528	0	0	0	0	0	0	0.05	νC=C[32]
1496	0	0	0	0	0	0.06	0	OC–CO[17]
1472	0	0.05	0	0.06	0.05	0	0	ν_sC-O[37]
1456	0.07	0.06	0	0.08	0	0.06	0.06	OH[55]
1420-1419	0.06	0	0	0.08	0.06	0.06	0.07	COO^-[40]
1398	0	0.06	0.07	0	0	0	0.06	νC=C[54]
1395	0.05	0	0	0.05	0	0	0	O=C-O^-/δ(C-C)[17,70]
1390	0	0	0	0	0	0.06	0	νOH[71]
1368	0.05	0	0	0	0	0	0	βOH[43]
1323	0	0	0	0.05	0.03	0	0	ν(C–C)[72]
1258-1256	0.06	0.06	0	0	0.05	0	0	COC[64]
1253-1249	0	0	0.05	0.08	0	0.05	0.05	νC-O[73]

Table S4: Correlation table for peaks, relative intensity, and position from PiF-IR of the small NGQD.

Particle No. / Wavenumber	1	2	3	4	5	6	7	Group
1773	0	0.04	0	0.08	0.05	0.06	0.09	νC=O[74]
1734	0.088	0.04	0.07	0.08	0.06	0.1	0.12	νC=O[10]
1718	0.099	0.09	0.09	0.08	0.06	0.09	0.18	νC=O[13]
1700	0.33	0.27	0.26	0.27	0.31	0.27	0.65	C=O[75]
1685	0.23	0.16	0.2	0.27	0.17	0.28	0.3	νC=O/ νC=C[16,76]
1653	1	1	1	1	1	1	1	νC=C[6,77]
1647	0.16	0	0	0	0	0	0	νC=O[77,78]
1636	0.19	0.13	0.15	0.2	0.15	0.18	0.27	νC=O/ νC=C[21,49,79]
1623	0.21	0	0.16	0.25	0.15	0.2	0.33	δOH[21]
1570-1560	0	0.1	0	0.17	0.12	0.13	0.19	δN-H & νC-N[80]
1541-1540	0.16	0.1	0.12	0	0.11	0.16	0.27	ν NH &CN/νC-C[81,82]
1473	0.16	0.09	0.11	0.16	0.13	0.14	0.21	CH_3[83]
1450	0	0.09	0	0.16	0	0	0	C-O[80]
1437	0	0.1	0.11	0	0	0	0.24	δCH_3/ν_{as}O-C-O[39,84]
1420	0.18	0.12	0.14	0.23	0.14	0.19	0.22	COO^- [40]
1354	0.18	0.11	0.1	0.19	0.15	0.15	0.23	C=N/phenazine[85]
1244	0.05	0.04	0.05	0.06	0.05	0.06	0.1	C=O[86]

Table S5: Correlation table for peaks, relative intensity, and position from PiF-IR of the medium NGQD.

Particle No. / Wavenumber	1	2	3	4	5	6	7	Group
1778	0	0	0	0.09	0	0	0.11	νC=O[3]
1770	0	0	0	0.09	0	0.13	0	νC=O[87]
1755	0	0	0.11	0	0	0	0	C=O[7]
1742	0.15	0.2	0.17	0.17	0.19	0.22	0.18	νC=O[9]
1734	0	0	0.11	0.12	0	0	0	νC=O[10]
1695	0.35	0.4	0.34	0.36	0.33	0.45	0.34	νC=O[6]
1684	1	1	1	1	1	1	1	νC=C[16,46]
1669	0.13	0.13	0.15	0.11	0.12	0.14	0.14	νC=O[18]
1660	0	0	0.17	0	0	0	0	νC=O & βN-H[88]
1649	0.12	0	0.08	0.1	0.12	0.13	0	νC=C[9]
1643	0	0	0	0	0	0	0.12	νC=O[47]
1629-1624	0	0.13	0	0.11	0.12	0.14	0.12	νC=O[29]
1591-1588	0	0.09	0	0.08	0.1	0	0.09	δNH_3[89]
1585	0.08	0	0	0	0	0	0	νC=C[25]
1574-1572	0.08	0	0	0	0.11	0	0	νC-N[15]
1570-1567	0	0	0	0	0	0	0.09	δN-H & νC-N[80]
1554	0	0	0	0	0	0.1	0	C=C[79]
1547-1545	0	0.11	0	0	0.09	0	0	νCN+δCHN/ C=N[29,46]
1536	0	0	0	0	0	0.09	0	δNH & νCN[90]
1514	0	0	0	0	0	0	0.07	νC-O [62]
1509	0	0	0	0	0	0.09	0	NH_2[91]
1490	0.06	0	0	0	0	0	0	νC=N[92]
1472	0.08	0	0	0	0.09	0.1	0.09	ν_sC-O[37]
1456	0.1	0.13	0.11	0.1	0.12	0.14	0.12	C−N/C=N[6]
1446	0	0	0	0	0	0.1	0	ν_a(C=N)[18]
1439	0	0	0	0	0.1	0	0	δCH_3[39]
1419	0.08	0.09	0.09	0.08	0.09	0	0.1	COO^-[40]
1395	0	0.09	0.07	0.08	0.1	0	0.09	O=C-O-/δC-C[17,70]
1372	0	0	0.06	0	0.08	0	0.07	OC–CO[17]
1337	0.04	0	0	0	0	0	0	CH_3CH_2O[61]
1332	0	0	0	0	0.05	0.06	0	
1301	0	0	0.05	0	0	0	0	C–N secondary aromatic amine[92]
1293	0	0	0	0	0	0.06	0	νC=O[93]
1251	0.06	0.09	0.09	0.09	0.08	0.09	0.08	νC-O[73]

Table S6: Correlation table for peaks, relative intensity, and position from PiF-IR of the large NGQD.

Particle No. / Wavenumber	1	2	3	4	5	6	7	Group
1779-1778	0.06	0	0	0	0	0	0.06	νC=O[3]
1763	0.06	0	0	0	0	0	0	νC=O[94]
1760	0	0	0	0	0	0	0.06	νC=O[6]
1747	0.06	0	0	0	0.16	0	0	νC=O/COOH[60]
1734	0.059	0.2	0	0	0	0.08	0.06	νC=O[10]
1718	0	0.15	0.13	0.27	0	0	0.06	νC=O[13]
1701-1700	0.06	0.25	0.3	0.41	0.35	0.11	0	C=O[75]
1685	0	0.23	0.13	0.42	0.31	0.11	0.1	νC=C/ νC=O[16,76]
1676	0.08	0	0	0	0	0.09	0	$\nu_{as}HCO_3^-$ [17]
1669	0	0	0	0	0.11	0	0	C=O[68]
1663	0	0	0.13	0.26	0	0	0.07	C=O[95]
1653	1	1	1	1	1	1	1	νC=C[6]
1635	0	0	0.08	0	0	0	0.06	νC=O[49,79]
1625-1623	0	0	0	0	0.11	0.04	0	δOH[21]
1602	0	0.13	0	0	0	0	0	oC-N[96]
1598	0	0	0	0	0.09	0	0	νC=C[97]
1570-1567	0	0	0	0.13	0	0	0	δN-H & νC-N[80]
1560-1559	0.05	0.11	0.15	0.14	0	0.05	0.07	δN-H & νC-N[80]
1558	0	0	0	0	0.14	0	0	νC-N[98]
1544	0	0.11	0	0	0	0	0	νCN+δCHN[46]
1541	0.048	0	0	0.18	0	0	0	νC-C[82]
1536-1534	0	0	0.07	0	0	0	0	δNH & νC-N[90]
1511	0.05	0	0	0	0	0	0	COOH[99]
1509-1507	0	0	0.07	0.18	0.15	0	0	NH_2/ν_{as}COOH[33,91]
1472	0	0	0	0	0.13	0.05	0	ν_sC-O[37]
1459-1456	0.06	0	0.08	0.16	0	0.05	0.07	C−N/C=N[6]
1438-1437	0	0	0	0.22	0	0.06	0	δCH_3[39]
1420-1419	0	0	0	0	0.11	0.05	0	COO^-[40]
1396	0	0	0.08	0	0	0	0	COH[100]
1386	0.052	0	0	0	0	0	0	C-N[101]
1354-1349	0.09	0.17	0.13	0.21	0.22	0.1	0.07	C=N/phenazine[85]
1338	0.05	0	0	0	0	0	0	δ/νOH[60]
1312	0.04	0	0	0	0	0	0	δ/νC-N[102]
1307	0	0	0	0.12	0	0	0	C-N[103]
1305	0	0	0	0	0	0.04	0	NH_4^+ [104]
1295	0	0	0	0	0	0	0.04	νC-O[105]
1259-1245	0.04	0	0.08	0	0.15	0	0	ν_{as}COC/C-N[35,65]
1228	0	0.14	0	0	0	0	0	N_{as}COC[106]

Table S7: Statistical analysis of spectral variability across the 94 GQD particles

Peak (cm^{-1})	**Mean (cm^{-1})**	**Standard Deviation (cm^{-1})**
1217-1223	1219.8	1.2

1252-1257	1253.8	1.0
1442-1447	1444.6	1.1
1457-1462	1459.8	1.0
1650-1658	1654.2	1.4
1682-1686	1684.1	0.7
1697.5-1701.5	1699.8	0.9
1717-1722	1719.4	1.0
1740-1744	1741.5	0.7

Table S8: Statistical analysis of intensity variability across 94 GQD particles

Peak (cm^{-1})	**Mean Intensity (a.u.)**	**Standard Deviation Intensity (a.u.)**
1220	8.46922E-6	5.99941E-6
1253	1.31354E-5	5.4036E-6
1445	1.72156E-5	1.09866E-5
1460	1.98768E-5	1.59078E-5
1654	2.32108E-5	2.02646E-5
1685	1.30733E-4	9.71286E-5
1700	3.27514E-5	1.62827E-5
1720	2.38648E-5	1.96598E-5
1742	2.30944E-5	8.66496E-6

Table S9: Statistical analysis of spectral variability across the 78 N-GQD particles

Peak (cm^{-1})	**Mean (cm^{-1})**	**Standard Deviation (cm^{-1})**
1353-1356	1353.9	0.7
1419-1421	1419.8	0.5

1506-1510	1507.9	1.0
1539-1543	1540.6	0.7
1558-1562	1559.6	0.9
1621-1628	1622.8	0.9
1651-1658	1653.4	1.0
1674-1678	1675.9	0.6
1683-1686	1684.7	0.43
1692-1698	1695.3	0.8
1697-1702	1699	0.5

Table S10: Statistical analysis of intensity variability across 78 GQD particles

Peak (cm^{-1})	**Mean Intensity (a.u.)**	**Standard Deviation Intensity (a.u.)**
1354	3.69281E-4	0.00259
1420	8.62776E-4	0.00703
1509	6.63215E-4	0.00551
1540	7.36637E-4	0.00603
1560	8.65876E-4	0.00722
1623	0.00118	0.00983
1653	0.00146	0.008
1676	0.00101	0.00846
1685	0.00301	0.02546
1696	0.00187	0.01612
1700	0.00175	0.01517

No	DFT predicted IR peak (cm^{-1})	IR peak position measured by PiF-IR (cm^{-1})	Group	Difference with respect to DFT (cm^{-1})	References
1.	1745	1750-1742	νC=O	-3 to +5	[9,60]
2.	1732	1735-1732	νC=O	0 to +3	[10]
3.	1695	1693	νC=O	-2	[6]
4.	1682	1684	νC=C	+2	[16]
5.	1664	1669	νC=O	+5	[18]
6.	1645	1653	νC=C	+8	[6]
7.	1617-1609	1613	CH	-4 to +4	[46]
8.	1575	1573	CH	-2	[46]
9.	1528	1524	C=C	-4	[32]
10	1418	1420	C=O	-2	[40]
11.	1376-1351	1375	OCHO	-1 to 24	[58]
12.	1266	1261	C-O	-5	[20]

Table S11: Comparison of IR spectra from DFT and PiF-IR of GQD

Table S12: Comparison of IR spectra from DFT and PiF-IR of NGQD

No	DFT predicted IR peak (cm^{-1})	IR peak position measured by PiF-IR (cm^{-1})	Group	Difference with respect to DFT (cm^{-1})	References
1.	1745	1747	νC=O	+2	[9]
2.	1736	1739-1734	νC=O	-3 to +2	[10]
3.	1720	1718	νC=O	-2	[13]
4.	1701	1700	νC=O	-1	[75]
5.	1680	1684-1675	νC=C	-4 to +5	[16]
6.	1662	1659	νC=O & βN-H	+3	[88]
7.	1653	1650	νC=C	-3	[6]
8.	1637-1623	1635-1623	νC=O	0 to +2	[49]
9.	1565	1559	δN-H & νC-N	+7	[80]
10.	1508	1509	NH_2/ν_{as}COOH	-1	[33,91]
11.	1476	1472	ν_sC-O	+4	[37]
12.	1433	1437	δCH_3	-4	[39]
13.	1420	1420	C=O	0	[40]
14.	1364-1346	1354	Phenazine	-4 to +10	[85]
15	1249	1244	ν_{as}COC/C-N	-5	[35]

Section 4: Optical Properties

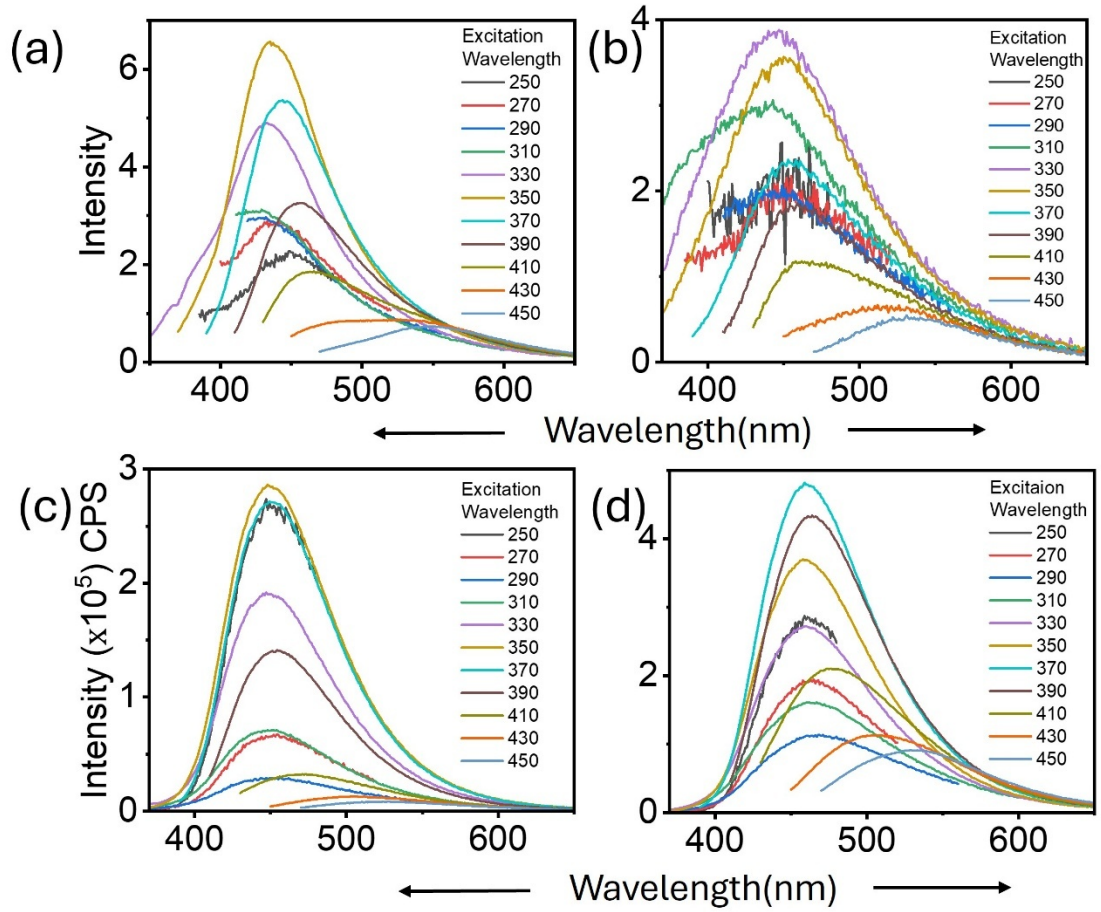

Figure S7: Normalized Emission at different excitation wavelength of (a) small, (b) medium GQDs and (c) Medium (d) Large NGQDs.

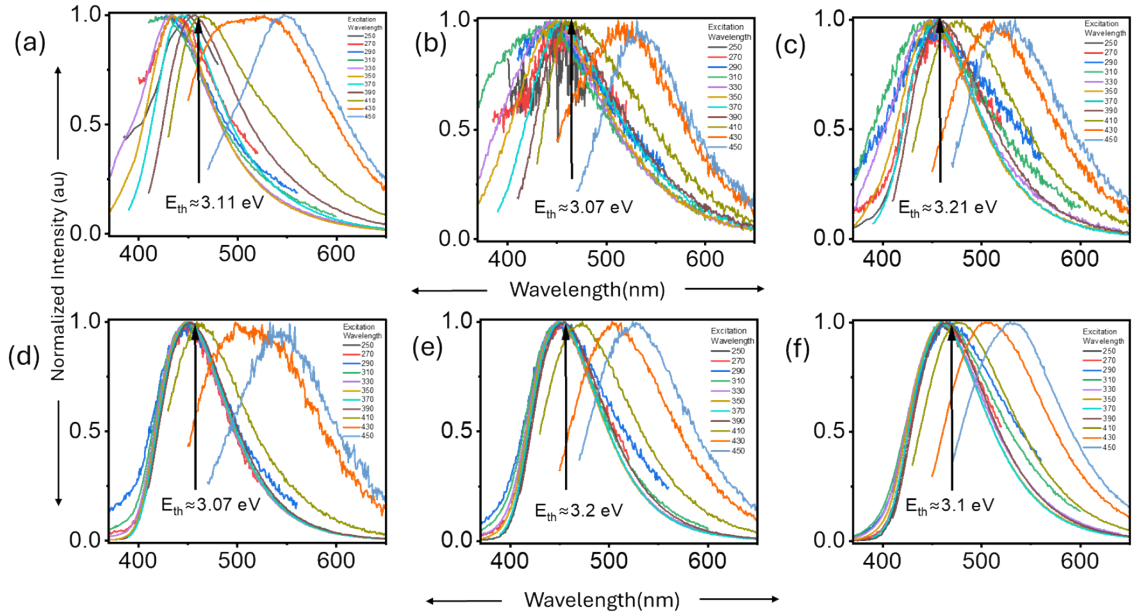

Figure S8: Normalized Emission at different excitation wavelength of (a) small, (b) medium, (c) large GQDs, and (d) small, (e) medium, (f) large NGQDs.

Table S13: Value of E_{th}

E_{th}(eV)	Large	Medium	Small
GQD	3.21	3.07	3.11
NGQD	3.1	3.2	3.07

Table S14: Parameters for exponential fit of time resolved photoluminescence spectra of GQDs

Large	Medium	Small
R_1^2=0.99	R_2^2=0.99	R_3^2=0.99
α_{11}=250	α_{21}=546	α_{31}=650
α_{12}=749	α_{22}=400	α_{32}=354
τ_{11}=3.4	τ_{21}=3.9	τ_{31}=3.4
τ_{12}=12.5	τ_{22}=11.4	τ_{32}=11.2
τ_{1avg}=12.5	τ_{2avg}=9.03	τ_{3avg}=8.4

Table S15: Parameters for exponential fit of time resolved photoluminescence spectra of NGQDs

Large	Medium	Small
R_3^2=0.99	R_2^2=0.99	R_1^2=0.99
α_{11}=4266	α_{21}=623	α_{31}=1583
α_{12}=1228	α_{22}=1717	α_{32}=481
τ_{11}=4.3	τ_{21}=5.6	τ_{31}=13.1
τ_{12}=14.8	τ_{22}=15.8	τ_{32}=20.3
τ_{1avg}=9.5	τ_{2avg}=14.7	τ_{3avg}=15.4

Section 5. Stability

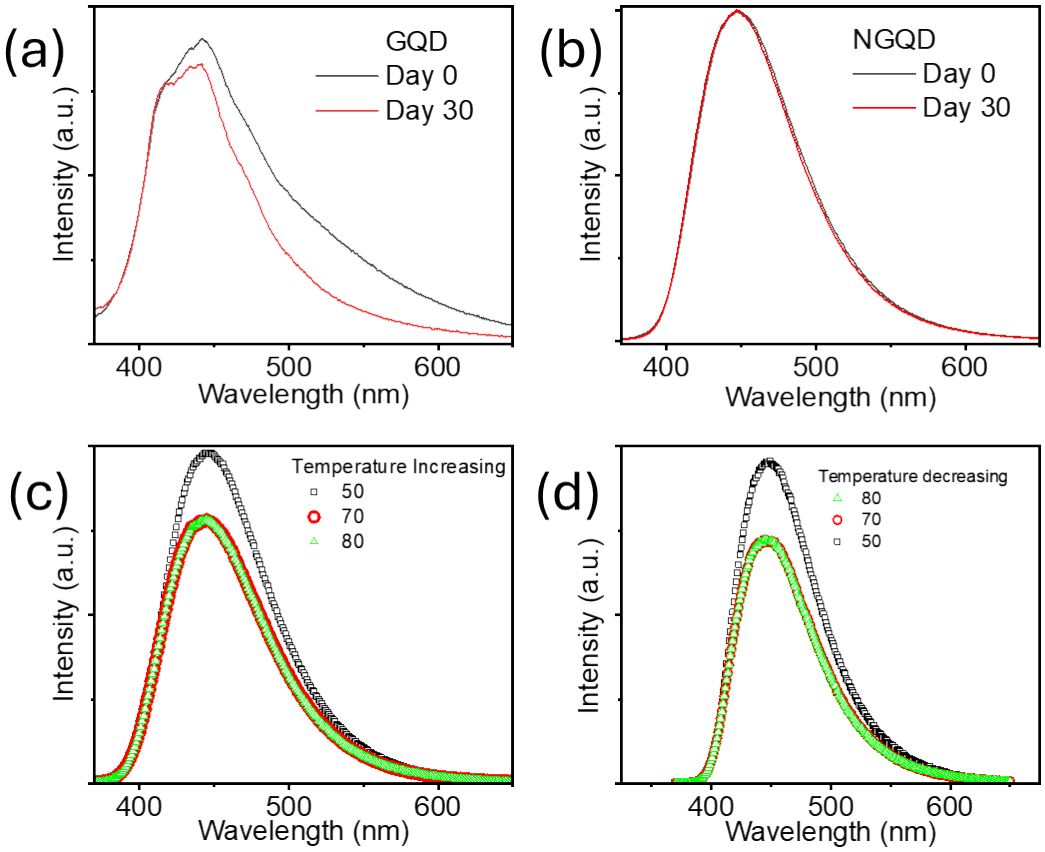

Figure S9: (a) Comparison of PL spectra of GQD one month apart. (b) Comparison of PL spectra of N-GQD one month apart. (c) Comparison of PL spectra of NGQD at increasing temperature. (d) Comparison of PL spectra of NGQD at decreasing temperature.

Reference

1 A. Engel, C.-A. Schoenenberger and D. J. Müller, *Curr Opin Struct Biol*, 1997, **7**, 279–284.

2 R. Mohammadkhani, M. Ramezanzadeh, S. Akbarzadeh, G. Bahlakeh and B. Ramezanzadeh, *Chemical Engineering Journal*, 2020, **397**, 125433.

3 S. Wang, N. Wang, D. Kai, B. Li, J. Wu, J. C. C. YEO, X. Xu, J. Zhu, X. J. Loh, N. Hadjichristidis and Z. Li, *Nat Commun*, 2023, **14**, 1182.

4 X. Li, P. Bandyopadhyay, T. T. Nguyen, O. Park and J. H. Lee, *J Memb Sci*, 2018, **547**, 80–92.

5 S. Pérez-Villar, P. Lanz, H. Schneider and P. Novák, *Electrochim Acta*, 2013, **106**, 506–515.

6 F. Rigodanza, M. Burian, F. Arcudi, L. Đorđević, H. Amenitsch and M. Prato, *Nat Commun*, 2021, **12**, 2640.

7 K. Liu, H. Qi, R. Dong, R. Shivhare, M. Addicoat, T. Zhang, H. Sahabudeen, T. Heine, S. Mannsfeld, U. Kaiser, Z. Zheng and X. Feng, *Nat Chem*, 2019, **11**, 994–1000.

8 Y. Fu, J. Wang, Q. Liu and H. Zeng, *Carbon N Y*, 2014, **77**, 710–721.

9 S. Pei, Q. Wei, K. Huang, H.-M. Cheng and W. Ren, *Nat Commun*, 2018, **9**, 145.

10 B. Shi, H. Wu, J. Shen, L. Cao, X. He, Y. Ma, Y. Li, J. Li, M. Xu, X. Mao, M. Qiu, H. Geng, P. Yang and Z. Jiang, *ACS Nano*, 2019, **13**, 10366–10375.
11 W. Hage, A. Hallbrucker and E. Mayer', *Carbonic Acid: Synthesis by Protonation of Bicarbonate and FTIR Spectroscopic Characterization via a New Cryogenic Technique*, 1993, vol. 115.
12 S. Li, W. Su, H. Wu, T. Yuan, C. Yuan, J. Liu, G. Deng, X. Gao, Z. Chen, Y. Bao, F. Yuan, S. Zhou, H. Tan, Y. Li, X. Li, L. Fan, J. Zhu, A. T. Chen, F. Liu, Y. Zhou, M. Li, X. Zhai and J. Zhou, *Nat Biomed Eng*, 2020, **4**, 704–716.
13 G. Niu, Y. Luan, J. Wang and H. Yang, *Advanced Devices & Instrumentation*, DOI:10.34133/adi.0039.
14 P. Yan, W. Zhao, F. McBride, D. Cai, J. Dale, V. Hanna and T. Hasell, *Nat Commun*, 2022, **13**, 4824.
15 R. Hestrin, D. Torres-Rojas, J. J. Dynes, J. M. Hook, T. Z. Regier, A. W. Gillespie, R. J. Smernik and J. Lehmann, *Nat Commun*, 2019, **10**, 664.
16 Y. Yamada, M. Kawai, H. Yorimitsu, S. Otsuka, M. Takanashi and S. Sato, *ACS Appl Mater Interfaces*, 2018, **10**, 40710–40739.
17 J. M. Wang, Q. Y. Zhu, J. H. Lee, T. G. Woo, Y. X. Zhang, W.-D. Jang and T. K. Kim, *Nat Commun*, 2023, **14**, 3808.
18 G. Zhan, L. Hu, H. Li, J. Dai, L. Zhao, Q. Zheng, X. Zou, Y. Shi, J. Wang, W. Hou, Y. Yao and L. Zhang, *Nat Commun*, 2024, **15**, 5918.
19 S. Wang, X. Yang, L. Hou, X. Cui, X. Zheng and J. Zheng, *Nat Commun*, 2022, **13**, 4401.
20 J. Wu, X. Wang, Q. Liu, S. Wang, D. Zhou, F. Kang, D. Shanmukaraj, M. Armand, T. Rojo, B. Li and G. Wang, *Nat Commun*, 2021, **12**, 5746.
21 C. Wei, Y. Fang, B. Liu, C. Tang, B. Dong, X. Yin, Z. Bian, Z. Wang, J. Liu, Y. Qian and G. Wang, *Nat Commun*, 2023, **14**, 3847.
22 H. Li, T. Lv, H. Sun, G. Qian, N. Li, Y. Yao and T. Chen, *Nat Commun*, 2019, **10**, 536.
23 C. Bartlam, S. Morsch, K. W. J. Heard, P. Quayle, S. G. Yeates and A. Vijayaraghavan, *Carbon N Y*, 2018, **139**, 317–324.
24 L. Wang, Y. Wang, T. Xu, H. Liao, C. Yao, Y. Liu, Z. Li, Z. Chen, D. Pan, L. Sun and M. Wu, *Nat Commun*, 2014, **5**, 5357.
25 B. Sui, Y. Zhu, X. Jiang, Y. Wang, N. Zhang, Z. Lu, B. Yang and Y. Li, *Nat Commun*, 2023, **14**, 6782.
26 Z. Lei, Q. Yang, Y. Xu, S. Guo, W. Sun, H. Liu, L.-P. Lv, Y. Zhang and Y. Wang, *Nat Commun*, 2018, **9**, 576.
27 H.-P. Cong, X.-C. Ren, P. Wang and S.-H. Yu, *Energy Environ Sci*, 2013, **6**, 1185.
28 X. Zhao, H. Lin, J. Li, L. Xin, C. Liu and J. Li, *Carbon N Y*, 2012, **50**, 3497–3502.
29 R. Shi, L. Liu, Y. Lu, C. Wang, Y. Li, L. Li, Z. Yan and J. Chen, *Nat Commun*, 2020, **11**, 178.
30 Z.-Z. Ma, Q.-H. Li, Z. Wang, Z.-G. Gu and J. Zhang, *Nat Commun*, 2022, **13**, 6347.
31 Y. Tang, S. Feng, L. Fan, J. Pang, W. Fan, G. Kong, Z. Kang and D. Sun, *Sep Purif Technol*, 2019, **223**, 10–16.
32 P. K. Srivastava, P. Yadav and S. Ghosh, *Nanoscale*, 2016, **8**, 15702–15711.
33 M. Jahan, Q. Bao, J.-X. Yang and K. P. Loh, *J Am Chem Soc*, 2010, **132**, 14487–14495.
34 R. Navik, Y. Gai, W. Wang and Y. Zhao, *Ultrason Sonochem*, 2018, **48**, 96–102.
35 Y. Wang, J. Yang, L. Wang, K. Du, Q. Yin and Q. Yin, *ACS Appl Mater Interfaces*, 2017, **9**, 20124–20131.
36 Z. Yang, Y. Zhu, X. Tan, S. J. J. Gunjal, P. Dewapriya, Y. Wang, R. Xin, C. Fu, K. Liu, K. Macintosh, L. G. Sprague, L. Leung, T. E. Hopkins, K. V. Thomas, J. Guo, A. K. Whittaker and C. Zhang, *Nat Commun*, 2024, **15**, 8269.
37 X. He, J. M. Larson, H. A. Bechtel and R. Kostecki, *Nat Commun*, 2022, **13**, 1398.
38 X. Feng, X. Zhao, L. Yang, M. Li, F. Qie, J. Guo, Y. Zhang, T. Li, W. Yuan and Y. Yan, *Nat Commun*, 2018, **9**, 3750.
39 W. Chen, K. A. Tarach, X. Yi, Z. Liu, X. Tang, K. Góra-Marek and A. Zheng, *Nat Commun*, 2022, **13**, 7106.

40 M. Wang, R. Wang, H. Yao, Z. Wang and S. Zheng, *RSC Adv*, 2016, **6**, 63365–63372.
41 S. Deng, Y. Zhang, A. H. Brozena, M. L. Mayes, P. Banerjee, W.-A. Chiou, G. W. Rubloff, G. C. Schatz and Y. Wang, *Nat Commun*, 2011, **2**, 382.
42 T. Van Khai, D. S. Kwak, Y. J. Kwon, H. Y. Cho, T. N. Huan, H. Chung, H. Ham, C. Lee, N. Van Dan, N. T. Tung and H. W. Kim, *Chemical Engineering Journal*, 2013, **232**, 346–355.
43 G. M. Morales, P. Schifani, G. Ellis, C. Ballesteros, G. Martínez, C. Barbero and H. J. Salavagione, *Carbon N Y*, 2011, **49**, 2809–2816.
44 M. Strankowski, D. Włodarczyk, Ł. Piszczyk and J. Strankowska, *Journal of Spectroscopy*, 2016, **2016**, 1–6.
45 P. A. Okafor and J. O. Iroh, *J Mater Chem A Mater*, 2015, **3**, 17230–17240.
46 V. Ţucureanu, A. Matei and A. M. Avram, *Taylor and Francis Ltd.*, 2016, preprint, DOI: 10.1080/10408347.2016.1157013.
47 Z. Chen, J. Wang, M. Hao, Y. Xie, X. Liu, H. Yang, G. I. N. Waterhouse, X. Wang and S. Ma, *Nat Commun*, 2023, **14**, 1106.
48 J. Zhang, X. Zhou, Q. Hu, K. Zhou, Y. Zhang, S. Dong, G. Zhao and S. Zhang, *Nat Commun*, 2024, **15**, 4265.
49 F. Sun, L. Liu, T. Liu, X. Wang, Q. Qi, Z. Hang, K. Chen, J. Xu and J. Fu, *Nat Commun*, 2023, **14**, 130.
50 C. Wei, Y. Fang, B. Liu, C. Tang, B. Dong, X. Yin, Z. Bian, Z. Wang, J. Liu, Y. Qian and G. Wang, *Nat Commun*, 2023, **14**, 3847.
51 S. Wang, K. Uwakwe, L. Yu, J. Ye, Y. Zhu, J. Hu, R. Chen, Z. Zhang, Z. Zhou, J. Li, Z. Xie and D. Deng, *Nat Commun*, 2021, **12**, 7072.
52 K. Anand, O. Singh, M. P. Singh, J. Kaur and R. C. Singh, *Sens Actuators B Chem*, 2014, **195**, 409–415.
53 Z. Xing, J. Tian, Q. Liu, A. M. Asiri, P. Jiang and X. Sun, *Nanoscale*, 2014, **6**, 11659–11663.
54 Z. Pei, L. Li, L. Sun, S. Zhang, X. Shan, S. Yang and B. Wen, *Carbon N Y*, 2013, **51**, 156–163.
55 A. Ghaffarkhah, S. A. Hashemi, S. Rostami, M. Amini, F. Ahmadijokani, A. Pournaghshband Isfahani, S. E. Mhatre, O. J. Rojas, M. Kamkar, S. Wuttke, M. Soroush and M. Arjmand, *Adv Funct Mater*, DOI:10.1002/adfm.202304748.
56 Y. Cui, Z. Huang, L. Lei, Q. Li, J. Jiang, Q. Zeng, A. Tang, H. Yang and Y. Zhang, *Nat Commun*, 2021, **12**, 5922.
57 Q. Ma, J. Song, C. Jin, Z. Li, J. Liu, S. Meng, J. Zhao and Y. Guo, *Carbon N Y*, 2013, **54**, 36–41.
58 X. Yu, Y. Xu, L. Li, M. Zhang, W. Qin, F. Che and M. Zhong, *Nat Commun*, 2024, **15**, 1711.
59 H. Li, T. Lv, H. Sun, G. Qian, N. Li, Y. Yao and T. Chen, *Nat Commun*, 2019, **10**, 536.
60 M. Manimehalai, P. Saranya, T. Theivasanthi and S. C. B. Gopinath, *Chemical Engineering Journal*, 2024, **496**, 154349.
61 X. Li, L. Li, X. Chu, X. Liu, G. Chen, Q. Guo, Z. Zhang, M. Wang, S. Wang, A. Tahn, Y. Sun and X. Feng, *Nat Commun*, 2024, **15**, 5639.
62 G. N. Vayssilov, M. Mihaylov, P. S. Petkov, K. I. Hadjiivanov and K. M. Neyman, *Journal of Physical Chemistry C*, 2011, **115**, 23435–23454.
63 J. Wu, X. Wang, Q. Liu, S. Wang, D. Zhou, F. Kang, D. Shanmukaraj, M. Armand, T. Rojo, B. Li and G. Wang, *Nat Commun*, 2021, **12**, 5746.
64 Y. Jiang, Q. Zhang, F. Li and L. Niu, *Sens Actuators B Chem*, 2012, **161**, 728–733.
65 C. Ingrosso, V. Valenzano, M. Corricelli, A. Testolin, V. Pifferi, G. V. Bianco, R. Comparelli, N. Depalo, E. Fanizza, M. Striccoli, A. Agostiano, I. Palchetti, L. Falciola and M. L. Curri, *Carbon N Y*, 2021, **182**, 57–69.
66 A. Ngqalakwezi, D. Nkazi, G. Seifert and T. Ntho, *Catal Today*, 2020, **358**, 338–344.
67 K. Pan, Y. Fan, T. Leng, J. Li, Z. Xin, J. Zhang, L. Hao, J. Gallop, K. S. Novoselov and Z. Hu, *Nat Commun*, 2018, **9**, 5197.

68 Y. Yang, Y. Chen, F. Izquierdo-Ruiz, C. Schäfer, M. Rahm and K. Börjesson, *Nat Commun*, 2023, **14**, 220.
69 Z. Wei, W. Shin, H. Jiang, X. Wu, W. F. Stickle, G. Chen, J. Lu, P. Alex Greaney, F. Du and X. Ji, *Nat Commun*, 2019, **10**, 3227.
70 Z. Jovanović, Ž. Mravik, D. Bajuk-Bogdanović, S. Jovanović, S. Marković, M. Vujković, J. Kovač, D. Vengust, S. Uskoković-Marković and I. Holclajtner-Antunović, *Carbon N Y*, 2020, **156**, 166–178.
71 Z. Wang, Y. Dong, H. Li, Z. Zhao, H. Bin Wu, C. Hao, S. Liu, J. Qiu and X. W. Lou, *Nat Commun*, 2014, **5**, 5002.
72 S. Amrollahi, B. Ramezanzadeh, H. Yari, M. Ramezanzadeh and M. Mahdavian, *Compos B Eng*, 2019, **173**, 106804.
73 A. Ngqalakwezi, D. Nkazi, G. Seifert and T. Ntho, *Catal Today*, 2020, **358**, 338–344.
74 L. Peng, J. Zhang, Z. Xue, B. Han, X. Sang, C. Liu and G. Yang, *Nat Commun*, 2014, **5**, 4465.
75 P. Yan, W. Zhao, F. McBride, D. Cai, J. Dale, V. Hanna and T. Hasell, *Nat Commun*, 2022, **13**, 4824.
76 J. Zhou, J. Li, L. Kan, L. Zhang, Q. Huang, Y. Yan, Y. Chen, J. Liu, S.-L. Li and Y.-Q. Lan, *Nat Commun*, 2022, **13**, 4681.
77 J. Chen, L. Li, J. Luo, L. Meng, X. Zhao, S. Song, Z. Demchuk, P. Li, Y. He, A. P. Sokolov and P.-F. Cao, *Nat Commun*, 2024, **15**, 6605.
78 L. Song, T. Zhu, L. Yuan, J. Zhou, Y. Zhang, Z. Wang and C. Tang, *Nat Commun*, 2019, **10**, 1315.
79 Q. Wu, H. Zou, X. Mao, J. He, Y. Shi, S. Chen, X. Yan, L. Wu, C. Lang, B. Zhang, L. Song, X. Wang, A. Du, Q. Li, Y. Jia, J. Chen and X. Yao, *Nat Commun*, 2023, **14**, 6275.
80 F. S. Ruggeri, G. Longo, S. Faggiano, E. Lipiec, A. Pastore and G. Dietler, *Nat Commun*, 2015, **6**, 7831.
81 K. Kanevche, D. J. Burr, D. J. Nürnberg, P. K. Hass, A. Elsaesser and J. Heberle, *Commun Biol*, 2021, **4**, 1341.
82 L. Tian, M. Su, F. Yu, Y. Xu, X. Li, L. Li, H. Liu and W. Tan, *Nat Commun*, 2018, **9**, 3642.
83 X. Sun, X. Chen, C. Fu, Q. Yu, X.-S. Zheng, F. Fang, Y. Liu, J. Zhu, W. Zhang and W. Huang, *Nat Commun*, 2022, **13**, 6677.
84 G. Zhang, T. Wang, M. Zhang, L. Li, D. Cheng, S. Zhen, Y. Wang, J. Qin, Z.-J. Zhao and J. Gong, *Nat Commun*, 2022, **13**, 7768.
85 J. Guo, Y. Xu, S. Jin, L. Chen, T. Kaji, Y. Honsho, M. A. Addicoat, J. Kim, A. Saeki, H. Ihee, S. Seki, S. Irle, M. Hiramoto, J. Gao and D. Jiang, *Nat Commun*, 2013, **4**, 2736.
86 W. Yuan, Y. Gu and L. Li, *Appl Surf Sci*, 2012, **261**, 753–758.
87 J. A. Prince, S. Bhuvana, V. Anbharasi, N. Ayyanar, K. V. K. Boodhoo and G. Singh, *Water Res*, 2016, **103**, 311–318.
88 D. Rodrigo, O. Limaj, D. Janner, D. Etezadi, F. J. García de Abajo, V. Pruneri and H. Altug, *Science (1979)*, 2015, **349**, 165–168.
89 J.-Y. Fang, Q.-Z. Zheng, Y.-Y. Lou, K.-M. Zhao, S.-N. Hu, G. Li, O. Akdim, X.-Y. Huang and S.-G. Sun, *Nat Commun*, 2022, **13**, 7899.
90 H. Sun and B. Marelli, *Nat Commun*, 2020, **11**, 351.
91 M. H. Abu Elella, E. S. Goda, H. M. Abdallah, M. M. Abdel-Aziz and H. Gamal, *Carbohydr Polym*, 2023, **303**, 120443.
92 S. Goswami, U. N. Maiti, S. Maiti, S. Nandy, M. K. Mitra and K. K. Chattopadhyay, *Carbon N Y*, 2011, **49**, 2245–2252.
93 C. Binet, A. Badri, M. Boutonnet-Kizlingt and J.-C. Lavalley, *FTIR Study of Carbon Monoxide Adsorption on Ceria: COZ-Carbonite Dianion Adsorbed Species*, 1994, vol. 11.
94 R. T. Pekarek, A. Affolter, L. L. Baranowski, J. Coyle, T. Hou, E. Sivonxay, B. A. Smith, R. D. McAuliffe, K. A. Persson, B. Key, C. Apblett, G. M. Veith and N. R. Neale, *J Mater Chem A Mater*, 2020, **8**, 7897–7906.

95 L. Hu, Q. Zhao, S. Huang, J. Zheng, X. Guan, R. Patterson, J. Kim, L. Shi, C.-H. Lin, Q. Lei, D. Chu, W. Tao, S. Cheong, R. D. Tilley, A. W. Y. Ho-Baillie, J. M. Luther, J. Yuan and T. Wu, *Nat Commun*, 2021, **12**, 466.
96 W. Xie, Q. Tang, J. Xie, Y. Fei, H. Wan, T. Zhao, T. Ding, X. Xiao and Q. Wen, *Nat Commun*, 2024, **15**, 38.
97 I. Matulková, P. Kovaříček, M. Šlouf, I. Němec and M. Kalbáč, *Carbon N Y*, 2017, **124**, 250–255.
98 V. Amoli, J. S. Kim, E. Jee, Y. S. Chung, S. Y. Kim, J. Koo, H. Choi, Y. Kim and D. H. Kim, *Nat Commun*, 2019, **10**, 4019.
99 M. Zhou, Z. Wang, A. Mei, Z. Yang, W. Chen, S. Ou, S. Wang, K. Chen, P. Reiss, K. Qi, J. Ma and Y. Liu, *Nat Commun*, 2023, **14**, 2473.
100 J. Guan, X. Chen, T. Wei, F. Liu, S. Wang, Q. Yang, Y. Lu and S. Yang, *J Mater Chem A Mater*, 2015, **3**, 4139–4146.
101 S. Kumar, P. Kumar, A. Deb, D. Maiti and S. L. Jain, *Carbon N Y*, 2016, **100**, 632–640.
102 Y. Hu, Z. Liu, C.-C. Wu, J. L. Gottfried, R. Pesce-Rodriguez, S. D. Walck, P. W. Chung and S. Ren, *Nat Commun*, 2021, **12**, 5696.
103 R. Qin, S. Li, Y. Qiu, Y. Feng, Y. Liu, D. Ding, L. Xu, X. Ma, W. Sun and H. Chen, *Nat Commun*, 2022, **13**, 1938.
104 S. D. Shraer, N. D. Luchinin, I. A. Trussov, D. A. Aksyonov, A. V. Morozov, S. V. Ryazantsev, A. R. Iarchuk, P. A. Morozova, V. A. Nikitina, K. J. Stevenson, E. V. Antipov, A. M. Abakumov and S. S. Fedotov, *Nat Commun*, 2022, **13**, 4097.
105 D. Wu, K. Luo, S. Du and X. Hu, *J Power Sources*, 2018, **398**, 99–105.
106 Y. Han, T. Wang, T. Li, X. Gao, W. Li, Z. Zhang, Y. Wang and X. Zhang, *Carbon N Y*, 2017, **119**, 111–118.